Magnesium Ferrite Spinels as Anode Modifier for the treatment of Congo red and Energy recovery in a Single Chambered Microbial Fuel Cell

Nishat Khan[1], Abdul Hakeem Anwer[1], Mohammad Danish Khan[1], Ameer Azam[2], Alex Ibhadon[3], Mohammad Zain Khan[1]*

[1]*Environmental Research Laboratory, Department of Chemistry, Aligarh Muslim University, Aligarh 202 002, UP, India*

[2]*Department of Applied Physics, Aligarh Muslim University, Aligarh 202 002, UP, India*

[3]*Department of Chemical Engineering, Faculty of Science and Engineering, University of Hull, Cottingham Road, Hull, United Kingdom HU6 7RX*

Abstract

Magnesium Ferrite (**$MgFe_2O_4$**) spinel structures prepared by a solid state reaction method was used as an anode modifier in the microbial fuel cell (MFC) treatment of Congo red dye. The performance of the reactors with unmodified stainless steel mesh anode (CR-1) and $MgFe_2O_4$ coated stainless steel mesh anode (CR-2), was accessed in terms of treatment efficiency, decolourisation efficiency, power density (PD) and columbic efficiency (CE). The microbial fuel cell treated Congo red wastewater was further treated aerobically in an activated sludge system. In this study, the peak PDs were observed to be 295.936 (CR-1) and 430.336 mW/m^2 (CR-2) respectively, revealing increased bioenergy output in the reactor with the $MgFe_2O_4$ modified anode, and indicating improvement in the extracellular electron transfer as compared to the unmodified stainless steel mesh anode. UV/Vis spectroscopy was used to confirm the biodegradation of the dye in the system. The final decolourisation efficiencies after the MFC and aerobic treatment of azo dyes, were found to be 87.918%, 92.053% for CR-1 and 92.010%, 98.386% for CR-2. The degradation products were further analyzed using Gas chromatography coupled Mass spectrometry system. Scanning electron

microscopy and energy dispersive X-ray mapping confirm a uniform coating of $MgFe_2O_4$ on the anode surface with evidence of biofilm formation associated with the growth of microbial community in the system. Electrochemical studies involving cyclic voltammetry confirmed the superior performance of spinel coated anode and the enhanced redox activity of the modified anode thereby improving the system performance. In addition, , the charge-discharge analysis confirmed the improved capacitive nature of the modified electrode improving the electrodes charge holding capacity. Thus, it can be concluded that a sequential anaerobic-aerobic process consisting of SCMFC coupled with the activated sludge downstream process, has the potential for low cost treatment of toxic and complex dyes with bioelectricity recovery.

Keywords- Activated sludge process, Azo dye, Bioelectrochemistry, Bioenergy, Ferrite spinel, Single chamber MFC

1. Introduction

Industrial processes such as chemical manufacturing, pulp and paper processing as well as textile operations in the past decades, have resulted in a significant increase in the discharge of toxic effluents into the environment. One of the most common effluents being discharged into aquatic bodies, regularly, are dye wastewaters from various industries ranging from textiles, pharmaceuticals, cosmetics, to paper and pigments. The scarcity of clean water across the world makes water pollution a major concern for human population as the increased volume of dye waste appreciably affect the aquatic ecosystems (Cao et al., 2010). In addition,, dye contaminated water released from industries is usually rich in colour, turbidity and chemical oxygen demand (COD) which have a significant adverse effect on the

aesthetics of fresh water (pH, temperature, opacity) with compromised quality and negative consequences on terrestrial and aquatic organisms (Khan et al., 2014). Azo dyes are one of the most common synthetic dyes that have been reported to be recalcitrant, toxic and mutagenic with high solubility in the aqueous environment and persistent nature (Huang et al., 2017a). The treatment of azo dyes is challenging as they generally show high stability towards heat, light and oxidation (Hou et al., 2011). Many physicochemical decolourisation and removal methods have been developed like reverse osmosis, flocculation, adsorption, electrolysis, neutralisation and many others, however, they suffer from limitations like production of toxic by-products, high operational cost, time consuming and complex processability (Ye et al., 2019; Ye et al., 2020; Bouras et al., 2019; Sathishkumar, K., 2019). For treatment processes such as membrane filtration, the high cost and potential fouling of membranes are major drawbacks and the resulting, filtrate discharge into the environment also presents a major concern. Similarly, adsorption also suffers from the issues of safe discharge of hazardous micropollutants (Kanaujiya et al., 2019). These limitations have made biological treatment a more favourable option for complete decolourisation of dye contaminated water with increased efficiency, ease of processability, environment feasibility and minimum secondary pollution (Roy et al., 2019). Bacterial communities among various microbes have been successfully employed to treat a wide variety of industrial and domestic wastewaters (Miranda et al., 2013; Paisio et al., 2012; Sharari et al., 2011). The utilisation of naturally existing microbes in lieu of external catalyst (physical or chemical) makes the biological treatment comparatively economical.

Studies have revealed that azo dyes can be degraded easily under anaerobic condition, making the anodic part of the MFC a feasible option for dye treatment. In a MFC, decolourisation of the azo dye and generation of electricity can be simultaneously

accomplished. The oxidation of the co-substrate by the bacteria present in the anodic chamber produces electrons which are utilised in two different ways by being accepted by the electrode to generate current or by the dye to be reduced and decolourised (Khan et al., 2017, 2019). The electron transfer process is the key factor in improving dye decolourisation and the MFC performance and the anode is the most important component of MFC controlling its overall performance (Huang et al., 2017a; Zhong et al., 2018). The shuttling of electrons between microbes and anode is known as extracellular electron transfer (EET) (Kumar et al., 2017). The electron transfer in MFC can occur via three different routes: short-range direct transfer, long-range direct transfer and indirect or electron transfer via mediators (Yong et al., 2017). The biofilm in direct physical contact with electrode takes active role in short-range direct transfer via involvement of outer membrane redox multiheme molecule called cytochrome c protein (Khan et al., 2017). Contrarily, for long-range direct transfer, multilayer biofilm can effectively conduct electrons via special pili-like electron carriers (nanowires) produced by exoelectrogens like *Geobacter* and *Shewanella spp.* (Kumar et al., 2015). Moreover, microbes can also transport electrons to anode via endogenous (microbially synthesised) mediators such as pyocyanin, riboflavin or exogenous (externally added) mediators such as 2,2'-azino-bis(3-ethylbenzothiazoline-6-sulphonic acid) (ABTS) and ferricyanide (Kumar et al., 2015; Malvankar and Lovley 2014; Zhang et al., 2011). Thus, in order to achieve efficient EET, microbe-anode compatibility is a crucial criterion. An ideal anode material should be low cost and biocompatible with improved electron transfer efficiency (Khilari et al., 2015a). A variety of carbon based materials (e.g. carbon paper, cloth felt, graphite plate or rod) have been widely used as MFC anodes but they present the major drawback of low conductivity which can be a major obstacle in up scaling of the technology (Lamp et al., 2011; Zheng et al., 2015). Also, the carbon based electrodes tend to be more

brittle making their durability limited (Lamp et al., 2011). Metal alloys such as stainless steel have been utilised in the limited number of studies as a potential anodic material because of its incredible conductivity, high stability and mechanical strength while being inexpensive and easily processable. However, this alloy has attained mixed reaction because of its limited current density output (Eyiuche et al., 2017). In general, traditional anode materials lag in electrochemical activity between anode and microbial communities and have been suggested to modify anode materials in bid to improve the extracellular electron transfer (Khilari et al., 2015a; Peng et al., 2017).

A variety of electrode modifiers have been used to improve the electron transfer efficiency and the MFC performance with the help of conducting polymers and metal oxides like PANI/carbon nanotube modified stainless steel electrode (Yellappa et al., 2019), Polypyrrole modified stainless steel (Pu et al., 2018), Iron-doped zinc oxide nanoparticles modified carbon paper electrode (Muthukumar et al., 2018), FeS_2 nanoparticle graphene electrode (Wang et al., 2018), PANI/TiO_2 modified carbon paper electrode (Yin et al., 2019), PANI/SnO_2 coated carbon cloth (Khan et al., 2020a).

Spinels are a special class of metal oxides with different valent cations. They are low cost, less toxic, and biocompatible with high conductivity, stability and electrochemical activity (Khilari et al., 2015a). Magnesium ferrite with n-type semiconducting properties exhibits cubic spinel and partially inverse spinel properties with the divalent and trivalent ions occupying tetrahedral and octahedral voids (Luo et al., 2017). Studies have revealed them to be environmental friendly depicting sufficient biocompatibility with non-toxic nature while being economically viable (Permien et al., 2015). As compared to bulk, nanosized $MgFe_2O_4$ particles have been reported to have improved properties with high electrochemical, electric and dielectric properties and high specific capacity (Luo et al., 2017; Narsimulu et al.,

2016). Spinel ferrites as nanocarriers have found numerous applications in biomedical sciences because of their biocompatibility and benign nature (Amiri et al., 2019). These properties make $MgFe_2O_4$ as a potential anode material. Exoelectrogens can utilise the ions commonly presents in spinels like Fe (III), Ni(II), Mg(II), or Co(II) as electron acceptors to improve biofilm development and electron transfer efficiency subsequently decreasing the internal resistance (Peng et al., 2017). Limited study has been performed studying the effect of spinel modifier on the traditional electrodes. Herein we studied the effect of magnesium ferrite ($MgFe_2O_4$) modified stainless steel mesh electrode on the performance of single chambered MFC treating Congo red dye. Performance of MFC in terms of power output and treatment efficiency was also evaluated. Electrochemical analyses were performed to elaborate the internal electrochemistry of the systems working with modified and unmodified electrodes.

2. Methodology

2.1. Synthesis of magnesium ferrite nanoparticles and electrode fabrication

The synthesis of magnesium ferrite ($MgFe_2O_4$) nanoparticles was performed with the help of solid state reaction method. $MgCO_3$ and Fe_2O_3 were taken in the molar ratio of 0.8:1 was mixed and grinded for 2 h with the help of mortar and pestle. Further the grounded powder was calcined in air for 10 h at 850 ºC. The calcined $MgFe_2O_4$ powder thus obtained was further grinded into fine powder (Kotnala and Shah, 2016).

The $MgFe_2O_4$ powder as catalyst and polyvinylidene fluoride (PVDF) in 10 % w/v as binder were mixed in 90:10 weight ratio in 1 mL N-methyl-2-pyrrolidone (NMP). The mixture was dispersed in ultrasonication bath for a period of 60 min. The electrospinning method was used to coat the stainless steel with the above prepared $MgFe_2O_4$ nanoparticles. The anode was positioned on top of the aluminium foil with a syringe hovering over it. An

electric field of 15 kV was applied across the syringe and aluminium foil to allow the fabrication of $MgFe_2O_4$ nanofibres on the stainless steel mesh at a constant flow rate of 0.5 mL/h for the $MgFe_2O_4$-binder composite mix. After an assortment time of 10 min, a successful fabrication of pink coloured $MgFe_2O_4$ nanofibres on stainless steel mesh was achieved. The as-synthesised $MgFe_2O_4$-electrode assembly was employed in the MFC reactor.

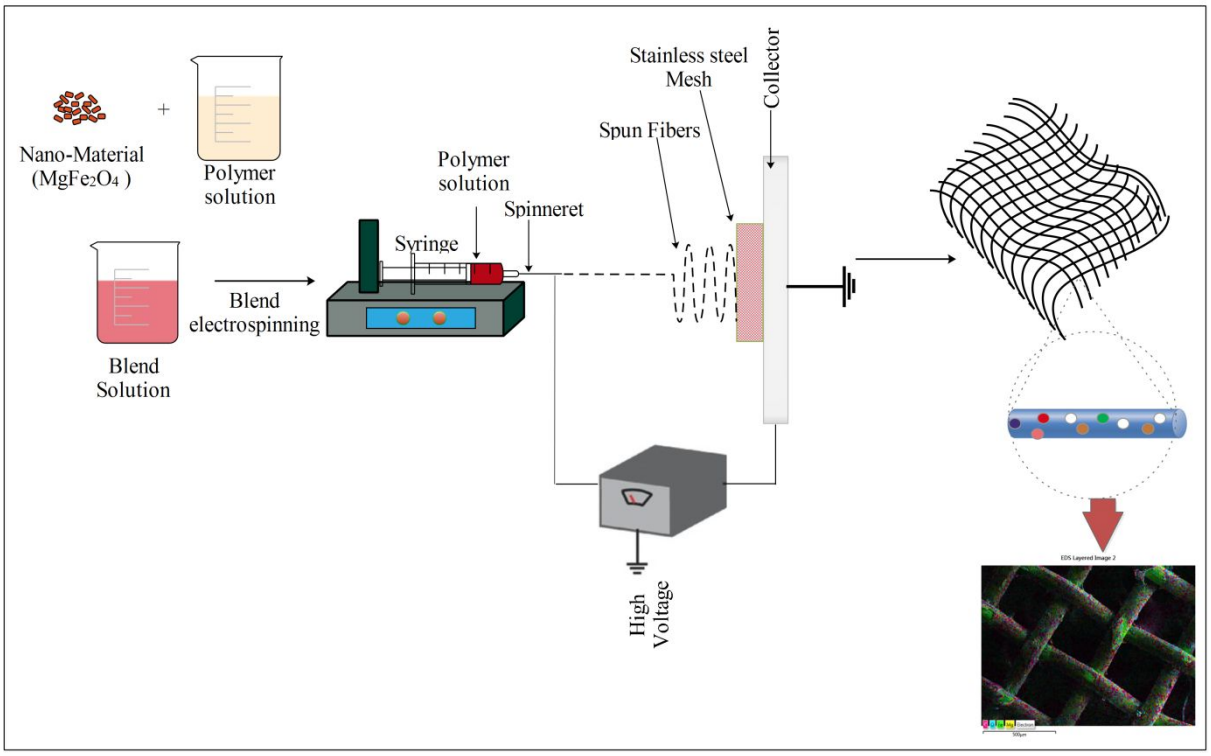

Fig. 1. Preparation and fabrication of $MgFe_2O_4$ nanofibres on stainless steel mesh electrode

2.2. Experimental Setups

Two single chambered microbial fuel cell (SCMFC) set-ups were made up of a plexi glass chamber with active volumes of 200 mL each were used in the present study under anaerobic conditions and designated as CR-1 (with plain anode) and CR-2 (with modified anode) Fig. 2. Stainless steel mesh (area 20 cm^2) were used as anode in both the reactors while carbon paper

cathode was placed on the outer surface of the plexi glass chambers and left open to air. In CR-1, plain stainless steel mesh anode was used while in CR-2, the $MgFe_2O_4$ modified stainless steel mesh was employed as anode for comparative analysis. The two electrodes were separated by a proton exchange membrane (PEM Nafion ®) placed on the opening of 1.5 cm diameter created on the wall of the plexi glass chamber. The electrodes were connected and the circuit was completed with the help of titanium wire having an external resistance of 500 Ω. The contents of the plexi glass chambers were continuously stirred with the help of a magnetic stirrer. The active volume of SMFC (200 mL) was filled in the ratio of 3:1 with 150 mL of dye wastewater and 50 mL of anaerobic sludge. A headspace of 50 mL was left in the reactor (total volume of reactors were 250 mL). Samples (4 mL) were collected at regular intervals (Khan et al., 2014).

The degradation products from MFC post treatment were light orange coloured and further treated in aerobic reactors to completely treat and decolourise the dye wastewater. The anaerobic reactors (SMFC) consisted of a 200 mL plexi glass chamber were left open to air. 150 ml of MFC effluent was transferred to the anaerobic reactor while the remaining 50 mL was left behind in MFC as anaerobic inoculum for the consecutive feed. The aerobic mixed liquor was aerated by a domestic air spurger (2 mL/s) in order to maintain the required dissolve oxygen level. The aerobic treatment was given for a period of 216 h. The aerobic post treatment process was employed to achieve complete degradation of the reduction products of azo-dyes (i.e. aromatic amines) however, since no significant change was observed after four days of aerobic treatment, the result was reported up to four days only.

Thus, MFC and aerobic treatment play their corresponding and significant role in treatment of Congo red dye. MFC plays a key role in treating the dye while generating electrical energy. The dye thus treated in MFC is broken down into aromatic amines (Dai et

al., 2020; Khan et al., 2015) which still pose threat to environment and need further treatment before the wastewater can be discharged in to natural water bodies (Dai et al., 2020; Khan et al., 2015). In an attempt to mitigate this, the effluent from MFC is treated in an aerobic downstream process that helps in breaking these aromatic amines to simpler compounds (Sultana et al., 2015).

2.3. Inoculation

The anaerobic and aerobic reactors were fed respectively with anaerobic and aerobic (return activated sludge) sludge collected from Okhla sewage treatment plant, New Delhi, India. The optical densities for the initial inocula were found to be 1.62 (for anaerobic) and 2.1 (aerobic culture). The composition of the synthetic media used in the SMFC consist of sodium acetate 1.0 g/L, NH_4Cl 0.85 g/L, KH_2PO_4 0.136 g/L, K_2HPO_4 0.234 g/L, $MgCl_2.6H_2O$ 0.084 g/L, $FeCl_3$ 0.05 g/L and Yeast extract 0.34 g/L to fulfil the micronutrient deficiency. Three different concentrations of Congo red dye (100, 200 and 300 mg/L) were fed to the SMFC for feasibility studies. The pH, temperature and conductivity remain 7–8.0, 30±2 °C and 10.8–15.7 mS/cm throughout the study (Khan et al., 2020b).

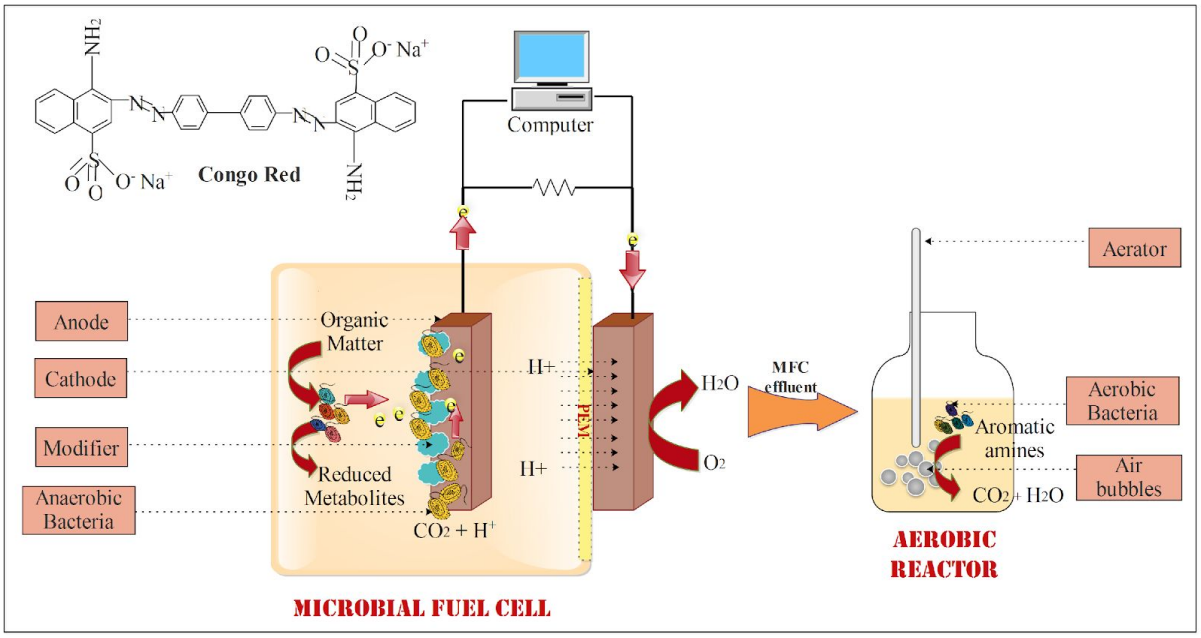

Fig. 2. Schematic diagram of the anaerobic-aerobic system used for the treatment of dye contaminated wastewater

3. Analytical methods

3.1. Material characterization

The as prepared magnesium ferrite anode modifiers were characterized by the power X-ray diffraction (XRD) in 2θ range of 5°-80° with Cu-Kα radiation, in order to confirm the crystal structure and particle size. Fourier transform infrared spectroscopy (FTIR Perkin Elmer) was also performed to study the bonding and presence of inorganic moieties in the as synthesized materials.

3.2. Monitoring MFC performance in terms of output energy and treatment efficiency

The output voltage across the external load was recorded with the help of a four channel data recording system (Kehao KH200, China). From the recorded voltage, the power density (PD) was calculated across the applied external resistance by using the following relation given below:

$$PD = \frac{V^2}{RA} \quad (1)$$

Coulombic efficiency is defined as ratio of the actual coulomb of charge transferred to the electrode and total number of coulombs transferrable when all the COD is converted to the electricity. CE of our system was calculated according to the formula given below:

$$C.E\% = \frac{M \int_0^t I.dt}{F.b.V_{an}.\Delta COD} \quad (2)$$

Where, M= Molar mass; I= current; t= time; F= Faraday constant (96485 C); b= no. of mol of electrons transferred per mol of COD; V_{an} = Volume of anodic chamber; ΔCOD= change in COD.

The decolourization efficiency of the dye was calculated using formula given below:

$$DE\% = \frac{A-B}{A} x100 \quad (3)$$

Where, A and B are initial absorbance and observed absorbance after treatment at λ_{max}.

Treatment of Congo red dye was confirmed with the help of UV/Vis spectroscopy by scanning the periodically collected sample in the range of 200-700 nm (Perkin Elmer Lambda 45, PerkinElmer, California, USA).

3.3 Degradation studies

The degradation of Congo red was ensured using Gas Chromatography coupled with Mass Spectrometry technique (Agilent GC-MS system ???? ?????). The GC contains DB capillary column coupled to MS detector with electron phase ionization mode using helium as carrier gas (I-Son Ng et al. 2013). The products of degradation were extracted from aqueous media

in ethyl acetate using 1:1 molar ratio and the contents were evaporated to improve the analyte concentrations. The following temperature program was employed- "initial column temperature was 45 °C for 3 min with a ramp of 10 °C per minute to 270 °C, held at 4 min and then again a ramp of 50 °C per minute to 280 °C, held at 5 min. The injector temperature was 220 °C. The molecular formula of the fragments was identified using NIST library.

3.4. Surface characterization of the anaerobic and aerobic microbial culture

The surface morphologies and elemental composition of the unmodified and $MgFe_2O_4$ coated anode were studied using a scanning electron microscopy (JEOL JSM-6510) coupled with an energy dispersive X-ray (EDX) system. The samples for SEM-EDX were prepared by firstly washing them with sodium cacodylate buffer followed by fixing overnight with 2% glutaraldehyde solution. The samples were later successively washed with graded ethanol (10, 30, 50, 80, 100 %) and dried under air.

3.5. Electrochemical analysis

The electrochemical activity in the MFC system was confirmed by cyclic voltammetry measurements using Electrochemical Analyzer (Autolab PGSTAT302N, Metrohm Autolab, Utrecht, Netherlands). The anode and cathode of MFC and standard Ag/AgCl electrode were designated as working, counter and reference electrodes respectively and the voltammograms were drawn at different rates 10 mV/s and 20 mV/s in the potential window of -1.0 to +1.0 V. The internal resistance of the MFCs were determined with the help of Electrochemical Impedance spectroscopy (EIS) performed using Electrochemical Analyzer (Autolab PGSTAT302N, Metrohm Autolab, Utrecht, Netherlands). The EIS analysis was conducted under two electrode systems with anode and cathode acting as working, counter and reference

electrodes over the frequency range of 10 KHz to 5 mHz under the OCV conditions with an amplitude of 10 mV.

4. Results and Discussion

4.1. FTIR spectra and X-ray diffraction

FTIR spectroscopy is a non-destructive technique that can be used to obtain information about the positions of the ions in the prepared nanoparticles. Fig. 3 (a) depicts the functional groups of $MgFe_2O_4$ recorded using FTIR spectroscopy in the frequency range 400–4000 cm^{-1} at room temperature. The broad bands ranging from 3437 to 3462 cm^{-1} are due to O–H vibrational modes. The band observed at 2932–2952 cm^{-1} is attributed to the C–H asymmetric stretching vibration mode (Tholkappiyan and Vishista, 2015). Another intense band is observed in the range from 1622 to 1631 cm^{-1}, and corresponds to a bending vibration mode of H–O–H in the ferrite. In Mg ferrites, the metal cations are situated at two different sub-lattices, namely the A-site (tetrahedral) and B-site (octahedral) positions. The C–O stretching modes from C–O-C group appear at 1035 cm^{-1}. The band at around 600 cm^{-1} is attributed to the stretching vibration mode of the tetrahedral complexes (A-site) and the band at around 400 cm^{-1} to that of the octahedral complexes (B-site) (Ahmad et al., 2018). Fig. 3(a) reveals two absorption bands at around 577 cm^{-1} and 432 cm^{-1}. The higher frequency band (577 cm^{-1}), is caused by the shorter bond length of metal oxygen stretching vibration on the tetrahedral site while the lower frequency band (432 cm^{-1}) can be assigned to longer bond length of metal oxygen stretching vibration on the octahedral site. The higher frequency bands υ_1 ranges from 581 to 612 cm^{-1} and the lower band υ_2 ranges from 405 to 422 cm^{-1} due to vibrations of Fe^{3+}─O_2 (metal–oxygen ions) in the stretching mode at the A-site and B-site positions which confirms the spinel structure of the prepared samples.

Fig. 3(b) shows the X-ray diffraction (XRD) pattern for magnesium ferrite sample. Result shows the spinel phase peaks having some impurity phase diffraction peaks also. All the characteristic peaks correspond to Fd-3m space group matches with JSPDS card no. 96-101-1242 of magnesium ferrite. Lattice constant of the composition has been calculated to be 8.38 by using the most intense peak (311). Crystallite size was estimated ~56 nm by using Debye Scherrer formula (Hussein et al., 2015).

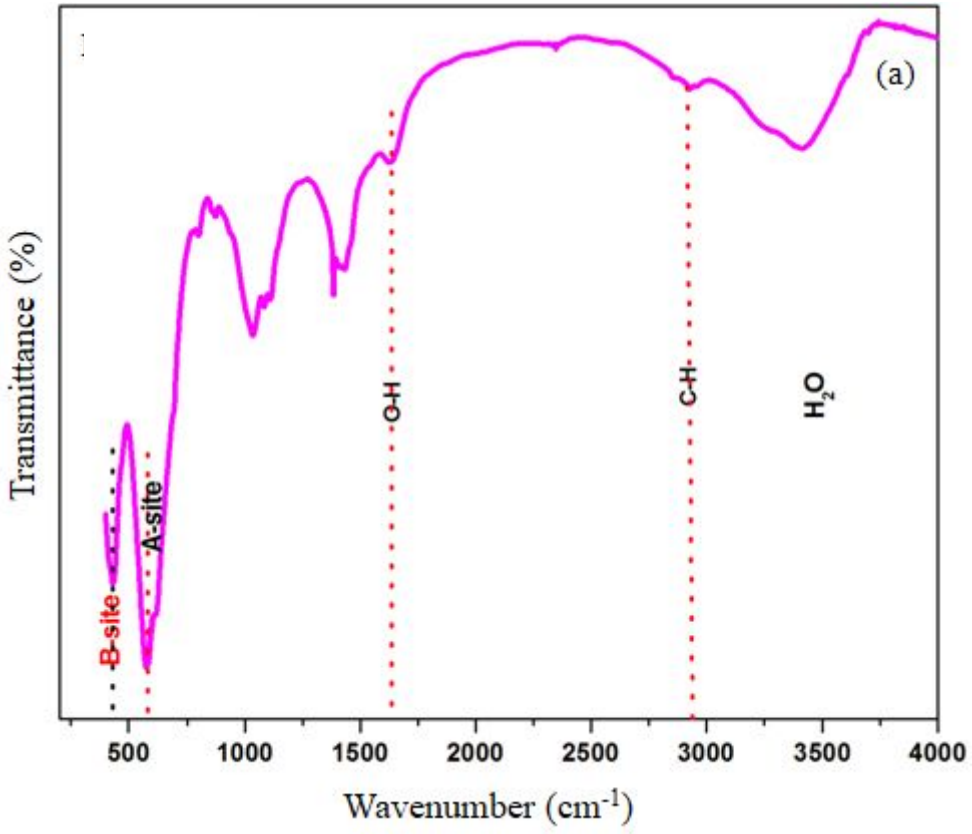

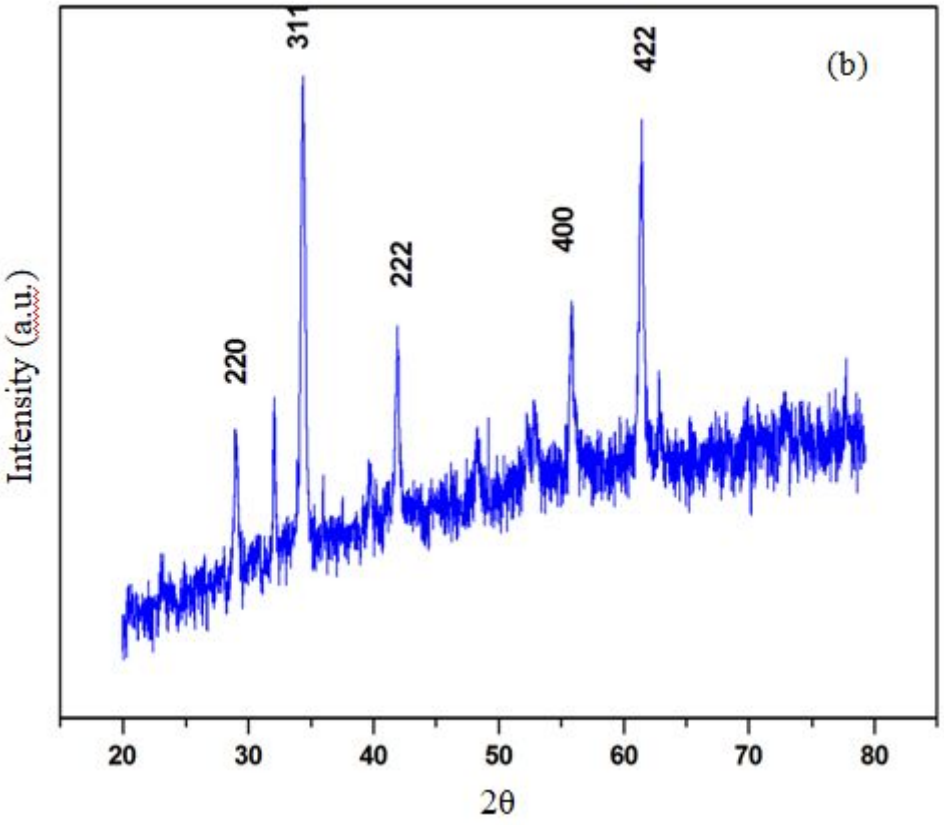

Fig. 3. (a) FTIR and (b) XRD spectra of as prepared magnesium ferrite spinel

4.3. Bioenergy generation in MFC

The voltage output for the MFC installed with unmodified (CR-1) and $MgFe_2O_4$ modified (CR-2) electrodes were recorded over time and presented in Fig. 4 (a-c). The voltage output increased with time and then become stable for all the Congo red concentrations tested. It was then observed to fall as the co-substrate was consumed by the microbial communities in the system. The fresh addition of co-substrate (acetate) boosted the voltage output for all the concentrations and followed the same trend. It was also observed for both the MFCs (CR-1 and CR-2) that the output voltage was highest for Congo red concentration of 100 mg/L and fell as the concentration increased systematically to 200 and 300 mg/L (Fig. 4 a-b). This fall in the voltage could be related to the increasing toxicity of Congo red dye affecting the

biofilm communities and thus the output performance of MFC. The maximum voltage output for MFC with the modified electrode was observed to be higher as compared to the unmodified electrode for all the concentration. Fig. 4c presents the comparative maximum voltage outputs of 544 mV for unmodified and 656 mV for $MgFe_2O_4$ modified MFC treating 100 mg/L of Congo red concentration.

The improvement in bioenergy could be attributed to increase in bacterial colonization on the surface of spinel coated anode, as also confirmed by SEM analysis. The increased bacterial colonization leads to the development of large negative anodic potential as the electrogens metabolize the substrate releasing more electrons. Electrogenic microorganisms like *Shewanella putrefacien* and *Geobacter metallireducen* are known to be capable of shuttling these electrons between substrate and Fe^{3+} via outer-membrane cytochromes initiating EET (Myers et al., 1990). The presence of these multivalent ions in $MgFe_2O_4$ improves EET which eventually leads to higher number of electrons reaching the anode and thus improves the voltage output (Khilari et al., 2015a).

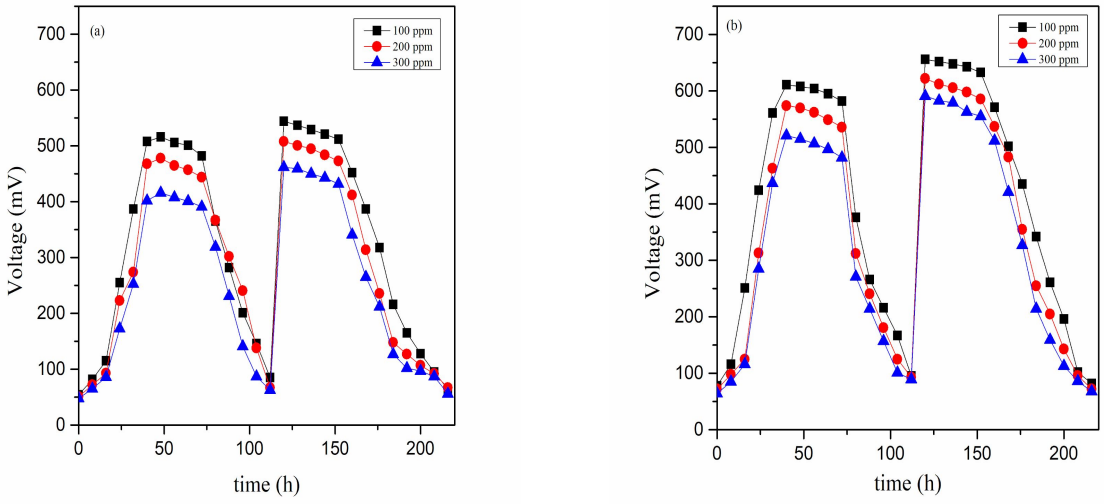

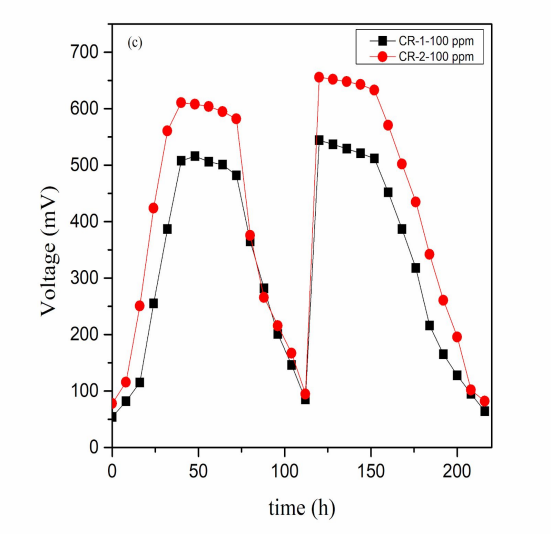

Fig. 4. Voltage output at the different dye concentrations for (a) CR-1 and (b) CR-2 MFC reactor and (c) comparative voltage at 100 ppm dye concentration

4.4. Power output and COD removal in MFC

The long term performance of MFC systems can be monitored and analysed in terms of power output and COD removal. Figs 5(a-c) present the power density and COD removal efficiency for both the reactors (CR-1 and CR-2) along with the comparative power output and COD removal at 100 ppm concentration. The maximum power densities for unmodified (CR-1) and $MgFe_2O_4$ modified (CR-2) MFCs were observed to be 295.936 and 430.336 mW/m^2 respectively for 100 mg/L dye concentration. The maximum power density for CR-2 was recorded to be nearly 150% of power density for CR-1. Similar to voltage output, the power density was highest for 100 mg/L concentration for both CR-1 and CR-2 and dropped as the concentration of Congo red was further increased. The observation emphasises on the importance of optimum concentration of substrate for higher output performance while maintaining appropriate food to famine ratio for the biofilm. The higher performance of CR-2 as compared to the CR-1 could be attributed to factors such as the increased surface area

improving microbial colonisation, improved nutrient transfer due to enhanced porosity, enhanced extracellular electron transfer due to the capacitive bridge created by $MgFe_2O_4$ nanoparticles. The multi-cation system in $MgFe_2O_4$ nanoparticles act as redox couple improving the electron transfer and eventually the performance of MFC similar to that of other reported spinels in literature (Munjal et al., 2020; Khilari et al., 2015a).

Furthermore, the maximum COD removal efficiency for CR-1 and CR-2 were found to be 89.419 and 92.285 % at the dye concentration of 100 mg/L. The COD removal efficiency was observed to follow the similar trend as power density and output voltage with highest removal efficiency at 100 mg/L of Congo red and decreases as the concentration of Congo red dye was increased in the MFC system. The trend can again be explained by considering the toxic effect of the increasing dye concentration on the microbial biofilm.

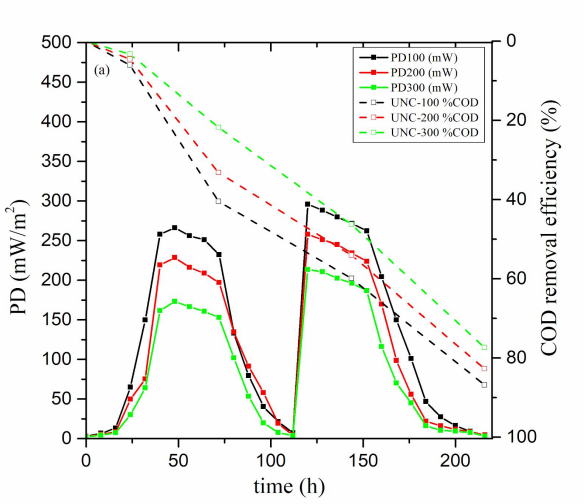

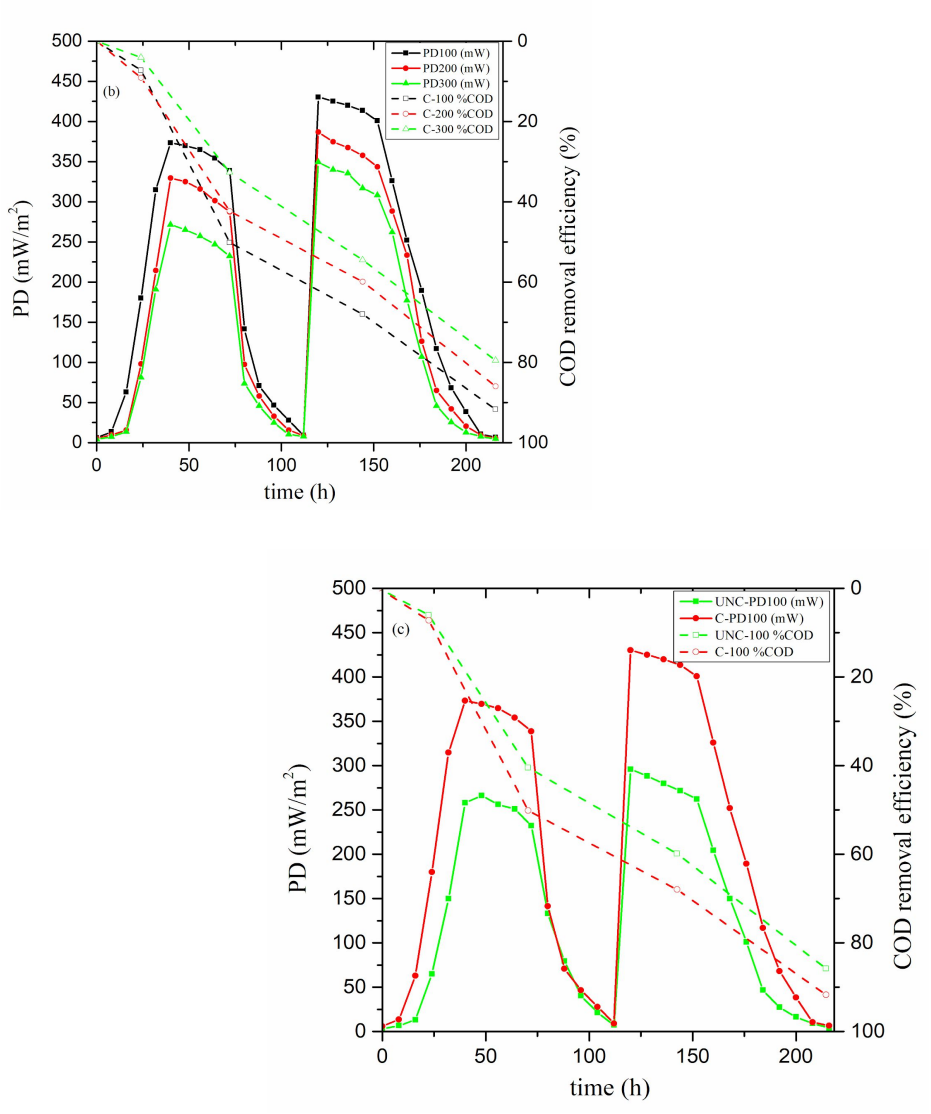

Fig. 5. Power densities and COD removal efficiencies at the different dye concentrations for (a) CR-1 and CR-2 MFC reactor and (c) at 100 ppm dye concentration

4.5. Coulombic performance of MFC system

Coulombic efficiency is the ratio of fraction of electrons transferred to the electrode. In the MFCs installed with unmodified and modified electrodes, the highest CEs over a 24 h period were found to be 1.913 and 2.543 % respectively. The CEs again followed a similar trend with highest efficiency at the lowest experimental concentration and falling as the concentration was stepwise increased. However, the CEs for modified anode were

consistently better as compared to the unmodified electrode for all the three test concentrations. Fig. 6 presents the comparative 24 h CEs for all the experimental dye concentrations for CR-1 and CR-2 respectively. The improvement in the CE of CR-1 as compared to the CR-2 can be correlated to the enhanced electron transfer efficiency and better biofilm development on the stainless steel anode decorated with $MgFe_2O_4$ as compared to the unmodified stainless steel anode due to its increased biocompatibility (Cardoso et al., 2018). The electron transfer process in MFC can occur in two ways either by transferring to anode for electricity generation or to the azo-dye for decolourisation. As the electrode modifier improves the electron shuttling by undergoing redox reactions continuously, the electron transfer is improved promoting the electron transfer rate between electrogens, anode and the dye molecules thereby improving both electricity generation and treatment efficiency in MFC (Huang et al., 2017b).

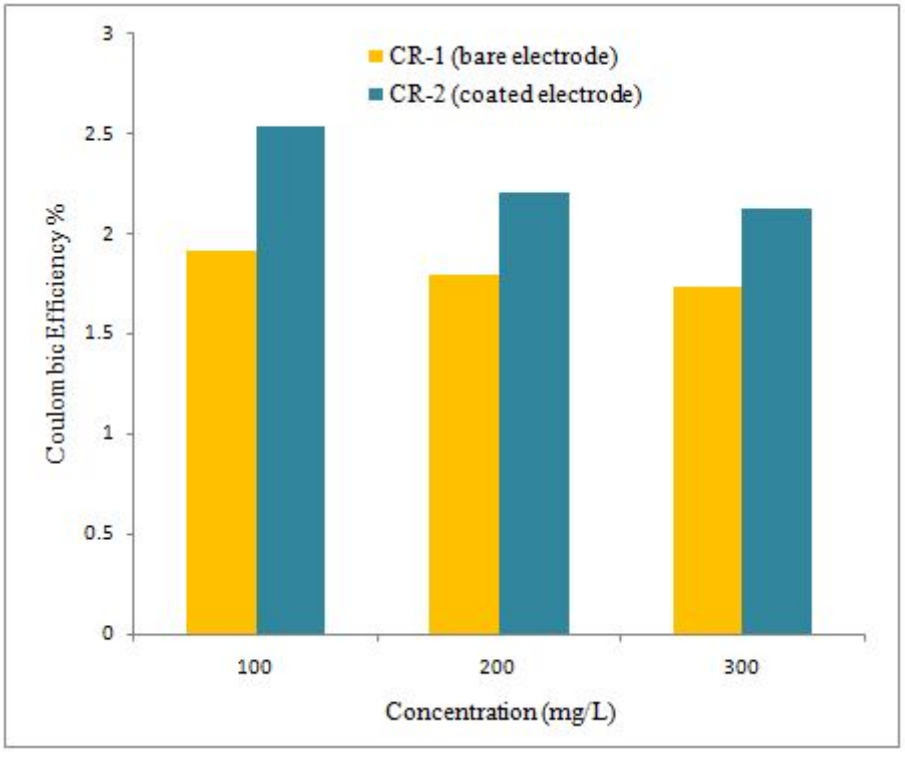

Fig. 6. Coulombic efficiency of Congo dye in CR-1 and CR-2 reactors

4.6. Degradation studies of Congo red dye in MFC

To examine the successful bio-electrodegradation of Congo red dye, UV/Vis spectroscopy was performed in the wavelength range of 200-700 nm (Fig. 7 a-b). The Congo red dye shows characteristics absorptions peaks at 240, 342 nm and 498 nm corresponding to benzene, naphthalene and azo bond (-N=N-) moieties respectively. The λ_{max} of 498 nm is attributed to the azo bonds of the dye and is responsible for colour. The change in the absorbance corresponding to 498 nm was monitored to ensure the treatment of Congo red successfully. Fig. 7a and b presents the absorption spectra for 100 mg/L concentration of Congo red dye for CR-1 and CR-2 respectively.

As can be seen from the graphs, after 10 days of treatment in the MFC system, about 85 % of dye was removed for CR-1 while for CR-2, nearly 88 % of the dye was removed during the same period. The decrease in the absorbance peak of azo group (λ_{max} 498 nm) and naphthalene moiety (λ_{max} 342 nm) confirms the treatment of the dye while the increase in the absorbance peak of benzene (240 nm) confirms the conversion of the complex dye into simpler phenyl components such as 8-Amino naphthol 3-sulfonic acid, p-diaminobipheny and p-Dihydroxy biphenyl as reported in previous works. (Cao et al., 2010; Dai et al., 2020, Telke et al., 2010). The anaerobic treatment transforms the azo dyes in to corresponding aromatic amines which are generally colorless due to absence of N=N bond. These aromatic amines are recalcitrant toward anaerobic treatment and are reported to undergo further degradation under aerobic conditions only. Thus, the effluent from the MFC reactors were further treated under aerobic conditions in activated sludge reactor to further decolourise and mineralize the degraded products of Congo red.

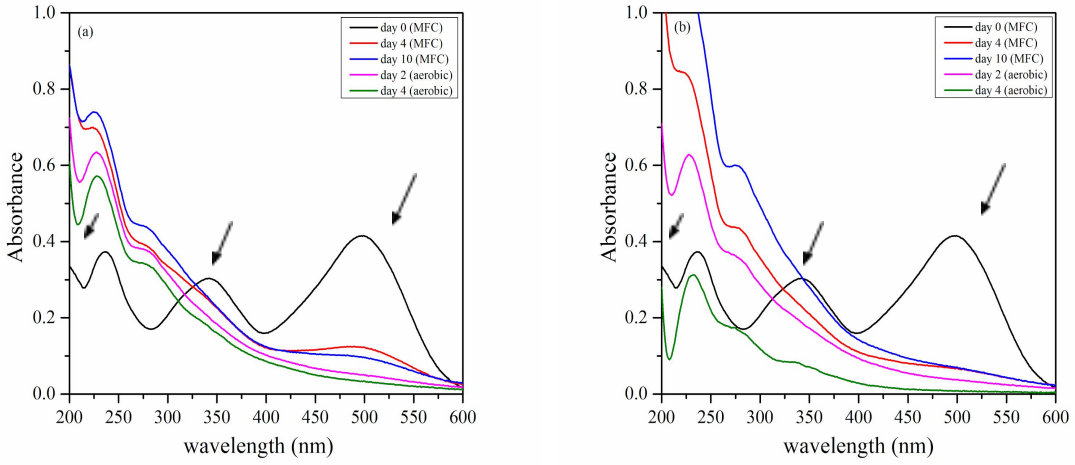

Fig. 7. UV/Vis spectra of pure, anaerobically and aerobically treated Congo red dye samples for (a)CR-1 and (b) CR-2

Fig. 7c. Proposed degradation pathway of Congo red dye under combined SCMFC treatment followed by activated sludge downstream process.

To further examine the biodegradation of Congo red and fate of its metabolite, GC-MS studies were carried out and the MS spectra are presented in Fig S1 (supplementary information). The degradation pathway of Congo red is well reported in literature and involves the formation of different metabolites (aromatic amines such as 8-Amino naphthol 3-sulfonic acid, p-diaminobipheny and p-dihydroxy biphenyl). Similar products were also formed in the present study and our results are in good agreement with those available in literature. For example, in the UV spectra there is a band corresponding to simple phenyl by-products at 240 nm which implies that it has been formed during Congo red degradation. In general, the reductive cleavage of azo bond produces naphthalenic moieties with hydroxyl, amino and sulfonic acid groups. These moieties were further degraded by deamination and desulfonation to form lower molecular weight compounds by the action of aerobic microorganisms. In order to strengthen our claim, GC MS analysis was done so as to confirm the formation of 8-Amino naphthol 3-sulfonic acid, p-diaminobipheny and p-dihydroxy biphenyl. Moreover, presence of characteristic peaks corresponding to carbonyl compounds in the vicinity of an acid group is also possible which show the formation of pthalic acid with ─C=O and ─COOH group undergoing hydrogen bonding. Based on GCMS data, a degradation pathway of Congo red under combined anaerobic-aerobic treatment has been proposed in Fig 7c. This again shows that 8-Amino naphthol 3-sulfonic acid, p-diaminobipheny and p-dihydroxy biphenyl, pthalic acid have been formed during the degradation of congo red in a combined anaerobic-aerobic process as has been reported by

other groups.

(This para will be finalized later. We are waiting for GCMS data. Rest all is done. A reaction pathway will be added in Fig.7c and the MS spectra of the degraded products will be added in the supplementary information.)

Thus, the study confirms that the sequential anaerobic-aerobic treatment involving SCMFC coupled with aerobic downstream process is a viable option for effectively treating complex azo dye substrates with simultaneous energy recovery in the form of bioelectricity. The decolourisation efficiency for dye treated in CR-1 and CR-2 for a period of 10 days was calculated from the absorbance observed at the λ_{max} of 498 nm before and after the treatment of dye and the highest decolourisation efficiency was observed to be 87.918 % and 92.010 % respectively. Most of the decolourisation was achieved within the first week of treatment of dye irrespective of the MFC setup. Bacterial azo dye reduction has been suggested by many researchers to involve electron transport chain on the outer membrane (Hong and Gu, 2010; Sydow et al., 2014). The improved decolourisation of azo dye in CR-2 as compared to CR-1 could be linked to the improved extracellular electron transfer due to the coating of spinel ferrite on the electrode surface thus improving the shuttling capability of the electron transport system between microbes and dye.

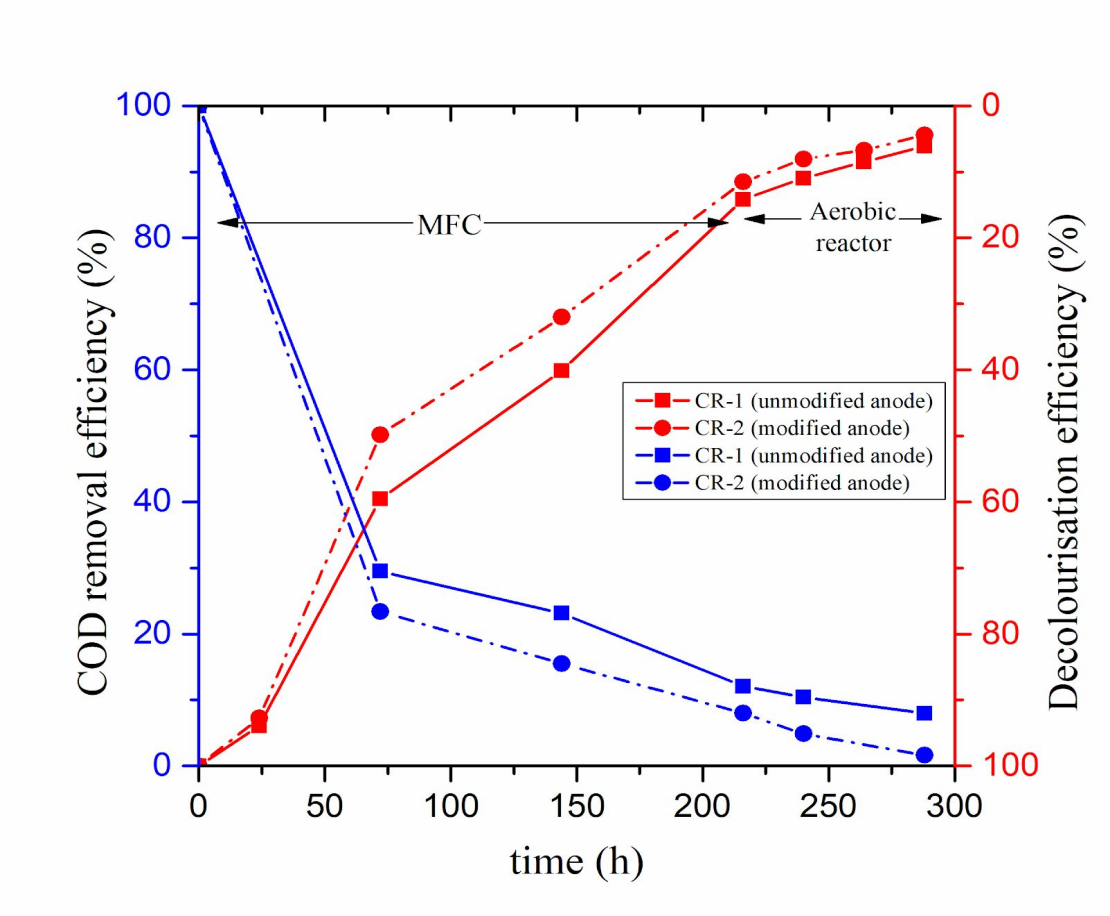

Fig. 8. COD removal efficiency (blue coloured) and decolourisation efficiency (red coloured) for 100 mg/L of dye sample treated in MFC and aerobic reactor respectively.

For complete removal of the metabolites of azo dyes (i.e. aromatic amines), the effluent from SCMFC were fed to an aerobic activated sludge reactor for 4 days which further reduces the colour of effluents coming from CR-1 and CR-2 MFC reactors to around to 92.053% and 98.386 % respectively. Thereafter, no prominent decolourisation was observed (after 4 days) in either of the reactors. Fig. 8 shows the COD removal (%) and decolourisation efficiency (%) for the 100 mg/L concentration of azo dye treated in MFC reactor followed by activated sludge reactor.

4.7. Microscopic analysis of the electrodes and biofilm

SEM coupled with EDX mapping was performed to confirm the uniformity of the $MgFe_2O_4$ on the surface of the stainless steel mesh electrode. Fig. 9 presents the SEM and EDX mapping images of the unmodified and modified anodes. As can be seen from the Fig. 9 (a-d), a uniform coating of $MgFe_2O_4$ was formed throughout the surface of the stainless steel mesh improving the available surface area of the electrode thereby enhancing the number of active sites for bioelectrocatalysis (Huang et al., 2017b). Fig. 9 (e,f) shows the SEM images of the unmodified and $MgFe_2O_4$ modified stainless steel mesh anode coated with the biofilm formed by the microorganisms involved in MFC under stable conditions. As can be seen from the images, different types of microorganisms (rod and spherical shaped) are dominant and involved in the biocatalysis (Ghasemi et al., 2016). The biofilm formed on the $MgFe_2O_4$ modified stainless steel mesh anode was perceived to be more porous as compared to the biofilm developed on the surface of unmodified stainless steel anode. The high porosity of biofilm can facilitate extracellular electron transfer in coated electrode as the deeper layers of biofilm can be involved in the electron transfer as compared to the dense and compact biofilm on the unmodified anode where electron transfer is limited to surface microbes due to mass and electron transfer limitations.

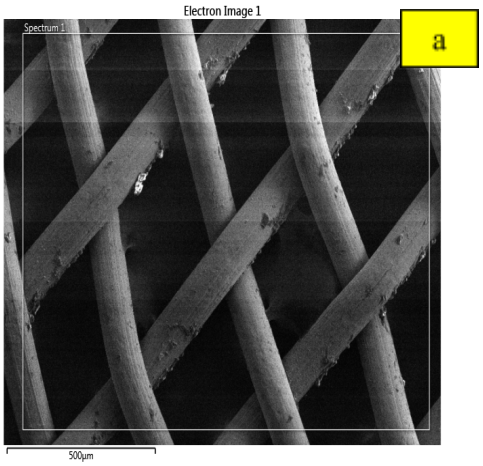

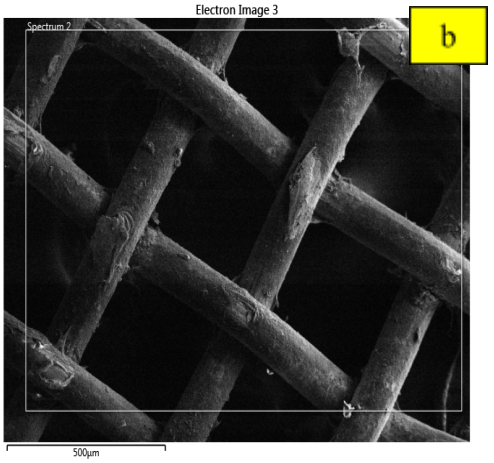

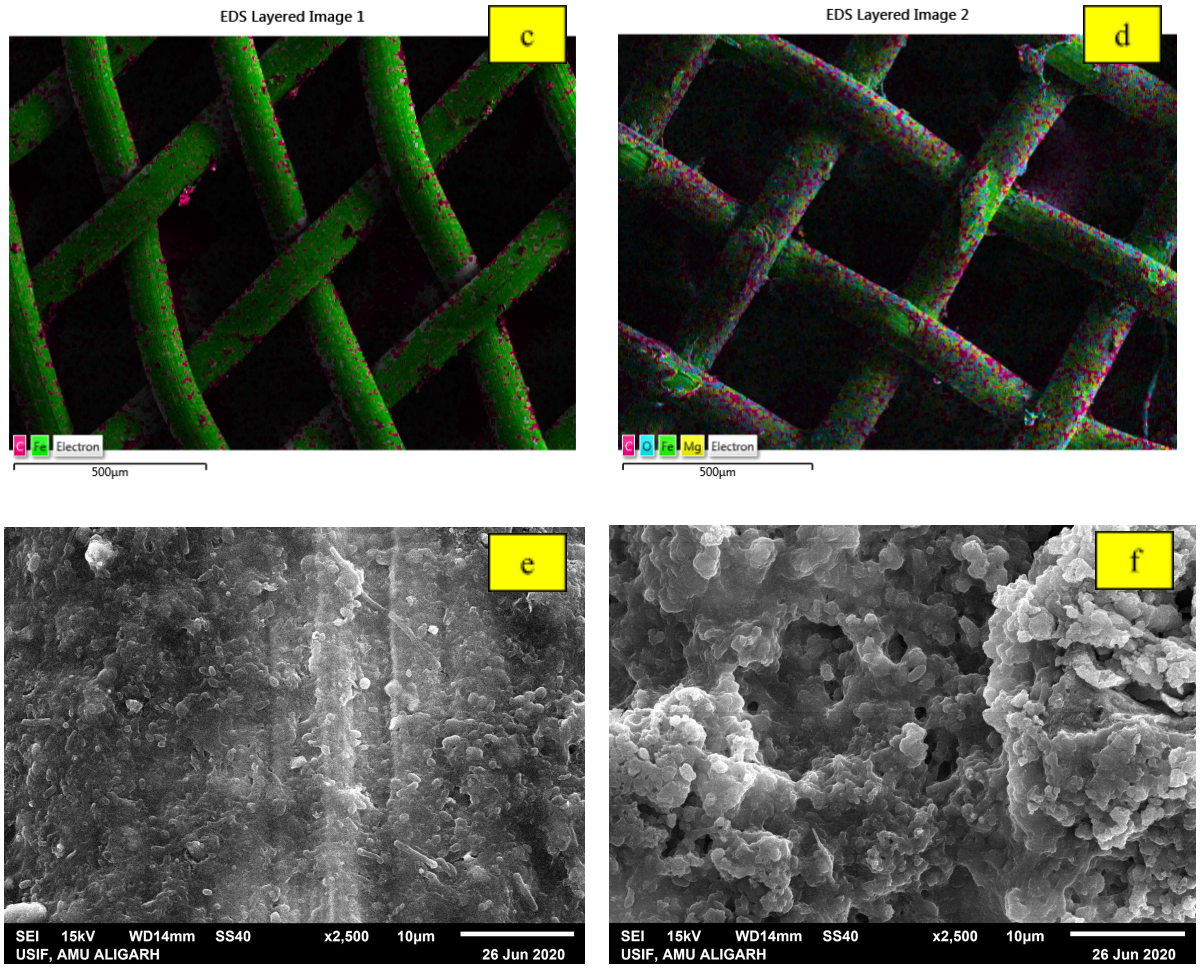

Fig.9. SEM images and EDS mapping of (a,c) unmodified; (b,d) $MgFe_2O_4$ coated stainless steel mesh anode and (e,f) biofilm coated modified and unmodified anodes

4.8. Electrochemical studies of the MFC setups

The two different experimental setups of MFC treating Congo red dye having unmodified and Mg ferrite modified anodes have been studied for the bioelectrochemical activities using cyclic voltammetry and the results have been presented in the Fig. 10. The voltammamograms for the comparative analysis were run at the scan rate of 10 mV/s and the results displayed one oxidation and two redox peaks for the dye being treated irrespective of the system. However, a slightly higher current intensity for CR-2 as compared to CR-1, indicated the superior performance of CR-2. The peak at around -0.5 V could be attributed to

the Congo red dye reduction as has also been suggested by Kong et al. with a potential shift being the result of difference in the electrode assembly. The other redox peak (at -0.3 and 0.08V) could be a related to the reversible reactions involving the intermediates formed during the bio-treatment like aromatic amines (Kong et al., 2014).

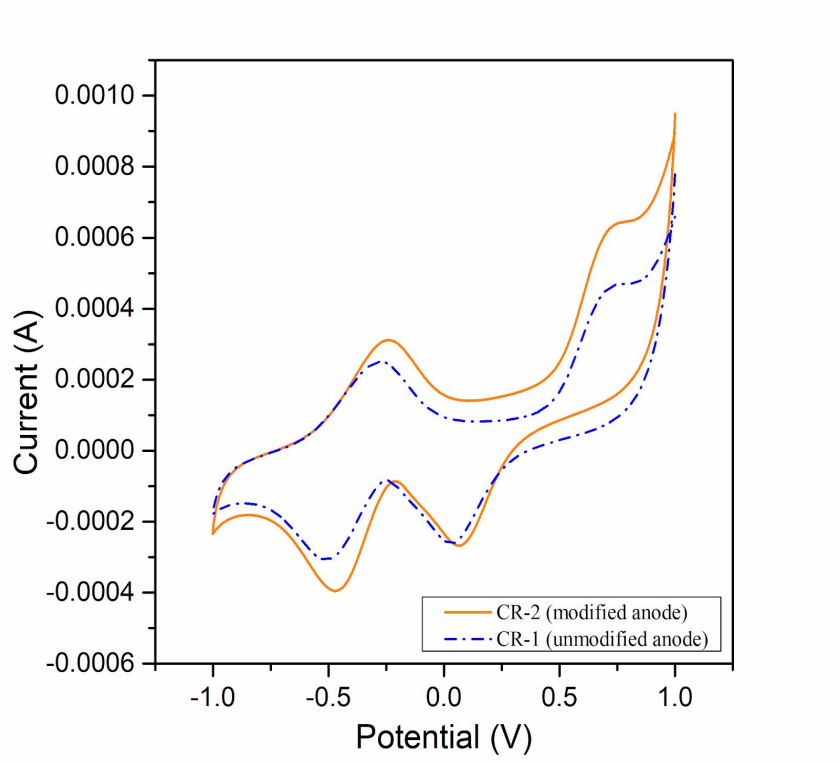

Fig. 10. Cyclic voltammograms of unmodified and modified (magnesium ferrite anode) anode

Furthermore, to investigate the role of anode modifier in improving the charge holding capacity of the electrode Galvanostatic charge-discharge analysis was performed. The galvanostatic charge-discharge profiles of the two MFCs were plotted and presented in Fig. 11. The charge-discharge capacity of stainless steel mesh was improved by applying a uniform coating of $MgFe_2O_4$ spinel. This implies that the $MgFe_2O_4$ coating played a vital role

in enhancing the charge storage capacity of the stainless steel mesh anode (Anwer et al., 2019; Khilari et al., 2015a).

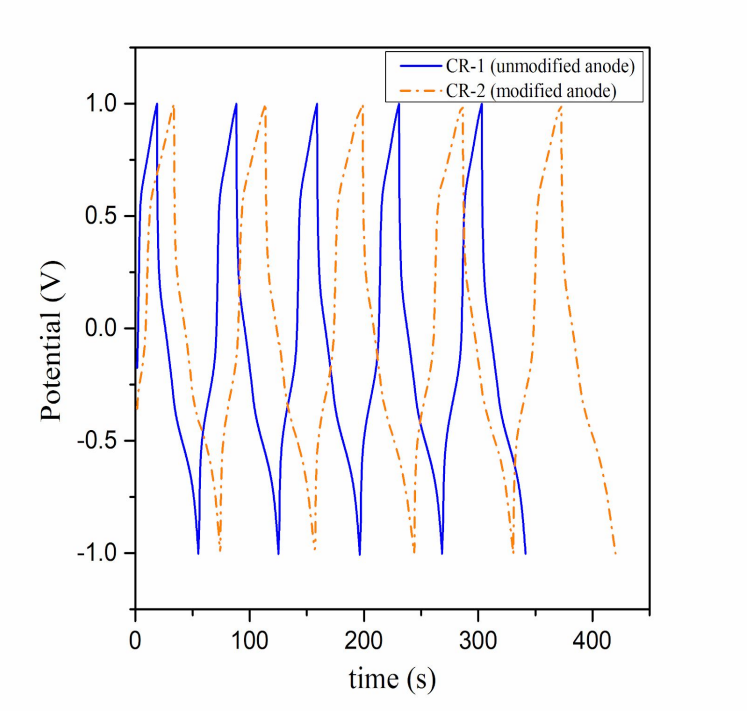

Fig. 11. Charging-discharging plot of MFC reactors with (a) unmodified and (b) magnesium ferrite modified anode

In order to further examine the charge and ion transfers within the MFC reactors, EIS analysis was performed. The measured impedance values were observed to influence the power output. The identical MFC reactor conditions were maintained to study the effect of changing anode on impedance keeping in mind the crucial role of biofilm-anode interaction in controlling the MFC performance. Nyquist plots were drawn to study the electron transfer resistance from different anodes under study (unmodified and $MgFe_2O_4$ modified stainless steel mesh anodes) (Fig. 12).

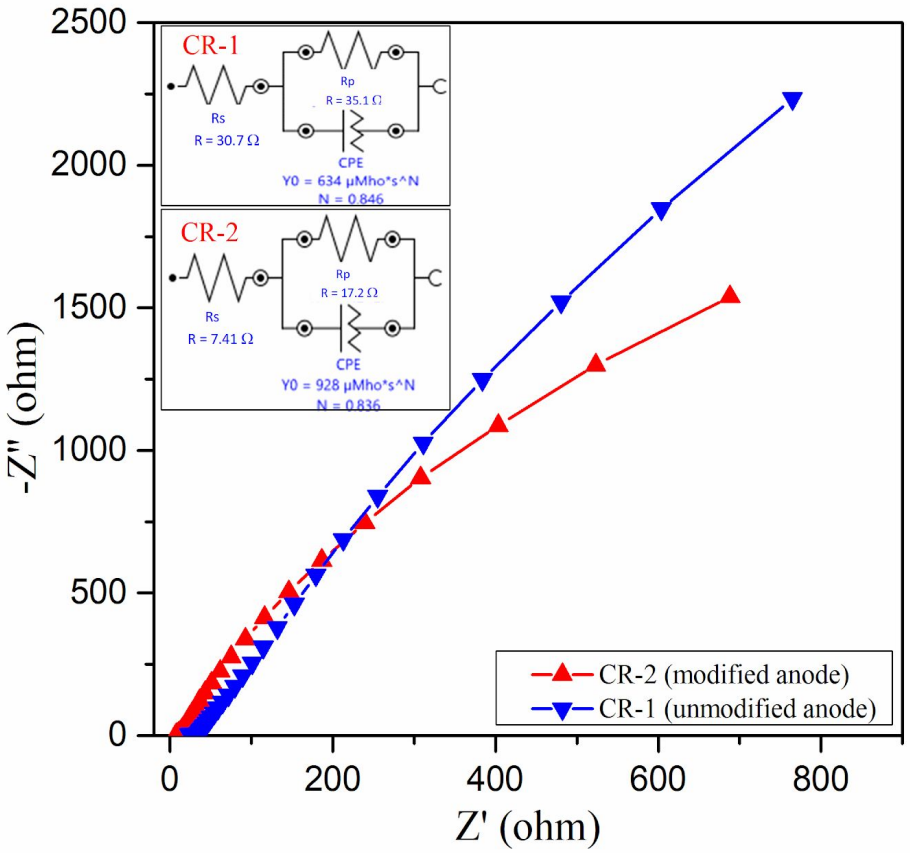

Fig. 12. Nyquist plot for spinel modified and unmodified stainless steel anode performing anaerobic treatment of azo dye

The results revealed lower ohmic resistance for modified electrode (7.41 Ω) as compared to the unmodified anode (30.7 Ω) suggesting enhanced conductivity of the modified anode. A similar trend was observed for charge transfer resistance which was observed to be approximately half of the value for modified electrode (17.4 Ω) compared to the unmodified electrode (35.1 Ω), again confirming the improved extracellular electron transfer between anode and biofilm and thus improving MFC performance (Yuan et al., 2016). The electrochemical studies thus confirmed the improved performance of spinel modified

stainless steel mesh anode over the unmodified stainless steel mesh anode in terms of dye removal and energy generation.

5. Conclusions

Successful biodegradation of Congo red dye was achieved following an anaerobic-aerobic protocol. The anaerobic treatment was performed in the microbial fuel cell followed by an aerobic activated sludge process. The results revealed better performance of modified anode as compared to the unmodified anode in MFC in terms of both treatment efficiency and energy generation with highest performance being obtained at the 100 mg/L dye concentration which decreases as the concentration was increased further. GC-MS studies further supported a combined anaerobic ─ aerobic approach for complete mineralization of Congo red dye. The cyclic voltammetry further confirmed superior performance while charge-discharge analysis indicated the higher capacitive nature of the modified electrode owing to improved surface area, better biocompatibility and higher extracellular electron transfer. EIS analysis established the improvement in performance of MFC due to the decreased ohmic and charge transfer resistances in MFC with modified anode. The study shows that ferrite could be used as potential electrode modifier for better performance of MFC.

Acknowledgments

The authors are thankful to Department of Chemistry, Aligarh Muslim University Aligarh for providing necessary research facilities. MZK and NK are also thankful to Science and Engineering Research Board (SERB), New Delhi for providing financial support to this work (EMR/2016/001896). Authors are also thankful to USIF, AMU Aligarh.

References

Ahmad, S.I., Ansari, S.A., Kumar, D.R., 2018. Structural, morphological, magnetic properties and cation distribution of Ce and Sm co-substituted nano crystalline cobalt ferrite. Mater Chem. Phys. 208, 248–257.

Amiri, M., Salavati-Niasari, M., Akbari, A., 2019. Magnetic nanocarriers: Evolution of spinel ferrites for medical applications. Adv. Colloid Interface Sci. 265, 29-44. doi.org/10.1016/j.cis.2019.01.003

Ng, I.S., Chen, T., Lin, R., Zhang, X., Ni, C., Sun, D. Decolorization of textile azo dye and Congo red by an isolated strain of the dissimilatory manganese-reducing bacterium *Shewanella xiamenensis* BC01. Appl Microbiol Biotechnol 98, 2297. doi:10.1007/s00253-013-5151-z.

Anwer, A.H., Khan, M.D., Khan, N., Nizami, A.S., Rehan, M., Khan, M.Z., 2019. Development of novel MnO_2 coated carbon felt cathode for microbial electroreduction of CO_2 to biofuels. J. Environ. Manage. 249, 109376. doi:10.1016/j.jenvman.2019.109376

Bouras, H.D., Isik, Z., Arikan, E. Z., Bouras, N., Chergui, A., Yatmaz, H.C., Dizge, N., 2019. Photocatalytic oxidation of azo dye solutions by impregnation of ZnO on fungi. Biochemical Engineering Journal 146, 150-159. doi.org/10.1016/j.bej.2019.03.014

Cao, Y., Hu, Y., Sun, J., Hou, B., 2010. Explore various co-substrates for simultaneous electricity generation and Congo red degradation in air-cathode single-chamber microbial fuel cell. Bioelectrochemistry 79, 71–76. doi:10.1016/j.bioelechem.2009.12.001

Cardoso, B., Rio, I.S.R., Rodrigues, A.R.O., Fernandes, F.C.T., Almeida, B.G., Pires, A., Pereira, A.M., J.P.Araujo, Castanheira, E.M.S., Coutinho, P.J.G., 2018. Magnetoliposomes containing magnesium ferrite nanoparticles as nanocarriers for the model drug curcumin. R. Soc. open sci. 5, 1–14. doi:10.1098/rsos.181017

Dai, Q., Zhang, S., Liu, H., Huang, J., Li, L., 2020. Sulfide-mediated azo dye degradation and microbial community analysis in a single-chambered air cathode microbial fuel cell. Bioelecrochemistry 131, 107349. doi.org/10.1016/j.bioelechem.2019.107349

Eyiuche, N.J., Asakawa, S., Yamashita, T., Ikeguchi, A., Kitamura, Y., Yokoyama, H., 2017. Community analysis of biofilms on flame-oxidized stainless steel anodes in microbial fuel cells fed with different substrates. BMC Microbiol. 17, 1–8. doi:10.1186/s12866-017-1053-z

Ghasemi, M., Wan Daud, W.R., Hassan, S.H.A., Jafary, T., Rahimnejad, M., Ahmad, A., Yazdi, M.H., 2016. Carbon nanotube/polypyrrole nanocomposite as a novel cathode catalyst and proper alternative for Pt in microbial fuel cell. Int. J. Hydrogen Energy 41, 4872–4878. doi:10.1016/j.ijhydene.2015.09.011

Hong, Y.G., Gu, J.D., 2010. Physiology and biochemistry of reduction of azo compounds by Shewanella strains relevant to electron transport chain. Appl. Microbiol. Biotechnol. 88, 637–643. doi:10.1007/s00253-010-2820-z

Hou, B., Sun, J., Hu, Y., 2011. Effect of enrichment procedures on performance and microbial diversity of microbial fuel cell for Congo red decolorization and electricity generation. Appl. Microbiol. Biotechnol. 90, 1563–1572. doi:10.1007/s00253-011-3226-2

Huang, W., Chen, Junfeng, Hu, Y., Chen, Jie, Sun, J., Zhang, L., 2017a. Enhanced simultaneous decolorization of azo dye and electricity generation in microbial fuel cell (MFC) with redox mediator modified anode. Int. J. Hydrogen Energy 42, 2349–2359.

Huang, W., Chen, Junfeng, Hu, Y., Chen, Jie, Sun, J., Zhang, L., 2017b. Enhanced simultaneous decolorization of azo dye and electricity generation in microbial fuel cell (MFC) with redox mediator modified anode. Int. J. Hydrogen Energy 42, 2349–2359. doi:10.1016/j.ijhydene.2016.09.216

Hussein, S.I., Elkady, A.S., Rashad, M.M., Mostafa, A.G., Megahid, R.M., 2015. Structural and magnetic properties of magnesium ferrite nanoparticles prepared via EDTA-based sol-gel reaction. J. Magn. Magn. Mater. 379, 9–15. doi:10.1016/j.jmmm.2014.11.079

Kanaujiya, D.K., Paul, T., Sinharoy, A., Pakshirajan, K., 2019. Biological Treatment Processes for the Removal of Organic Micropollutants from Wastewater: a Review. Curr. Pollut. Reports 5, 112–128. doi:10.1007/s40726-019-00110-x

Khan, M. D., Abdulateif, H., Ismail, I. M., Sabir, S., Khan, M. Z., 2015. Bioelectricity Generation and Bioremediation of an Azo-Dye in a Microbial Fuel Cell Coupled Activated Sludge Process. PLoS ONE 10 (10): e0138448. doi:10.1371/journal.pone.0138448.

Khan, M.D., Khan, N., Sultana, S., Joshi, R., Ahmed, S., Yu, E., Scott, K., Ahmad, A., Khan, M.Z., 2017. Bioelectrochemical conversion of waste to energy using microbial fuel cell technology. Process Biochem. 57, 141–158. doi:10.1016/j.procbio.2017.04.001

Khan, M.Z., Singh, S., Sreekrishnan, T.R., Ahammad, S.Z., 2014. Feasibility study on anaerobic biodegradation of azo dye reactive orange 16. RSC Adv. 4, 46851–46859. doi:10.1039/C4RA06716A

Khan, M. Z., Singh, S., Sultana, S., Sreekrishnan, T.R., Ahammad S. Z., 2015. Studies on the biodegradation of two different azo dyes in bioelectrochemical systems. New J. Chem. 39, 5597-5604. doi: 10.1039/c5nj00541h

Khan, N., Anwer, A.H., Ahmad, A., Sabir, S., Khan, M.Z., 2020a. Investigating microbial fuel cell aided bio-remediation of mixed phenolic contaminants under oxic and anoxic environments. Biochem. Eng. J. 155, 107485. doi:10.1016/j.bej.2019.107485

Khan, N., Anwer, A.H., Ahmad, A., Sabir, S., Sevda, S., Khan, M.Z., 2020b.

Investigation of CNT/PPy-Modi fi ed Carbon Paper Electrodes under Anaerobic and Aerobic Conditions for Phenol Bioremediation in Microbial Fuel Cells. ACS Omega 5, 471–480. doi:10.1021/acsomega.9b02981

Khan, N., Khan, M.D., Ansari, M.Y., Ahmad, A., Khan, M.Z., 2019. Bio-electrodegradation of 2,4,6-Trichlorophenol by mixed microbial culture in dual chambered microbial fuel cells. J. Biosci. Bioeng. 127, 353–359. doi:10.1016/j.jbiosc.2018.08.012

Khilari, S., Pandit, S., Varanasi, J.L., Das, D., Pradhan, D., 2015a. Bifunctional Manganese Ferrite/Polyaniline Hybrid as Electrode Material for Enhanced Energy Recovery in Microbial Fuel Cell. ACS Appl. Mater. Interfaces 7, 20657–20666. doi:10.1021/acsami.5b05273

Kong, F., Wang, A., Cheng, H., Liang, B., 2014. Accelerated decolorization of azo dye Congo red in a combined bioanode-biocathode bioelectrochemical system with modified electrodes deployment. Bioresour. Technol. 151, 332–339. doi:10.1016/j.biortech.2013.10.027

Kotnala, R.K., Shah, J., 2016. Green hydroelectrical energy source based on water dissociation by nanoporous ferrite. Int. J. Energy Res. 40, 1652–1661. doi:10.1002/er

Kumar, A., Hsu, L.H.H., Kavanagh, P., Barrière, F., Lens, P.N.L., Lapinsonnière, L., Lienhard, J.H., Schröder, U., Jiang, X., Leech, D., 2017. The ins and outs of microorganism-electrode electron transfer reactions. Nat. Rev. Chem. 1, 1–13. doi:10.1038/s41570-017-0024.

Kumar, R., Singh, L., Wahid, Z.A., Din, M.F.M., 2015. Exoelectrogens in microbial fuel cells toward bioelectricity generation: a review. Int. J. Energy Res. 39, 1048–1067. doi:10.1002/er.

Lamp, J.L., Guest, J.S., Naha, S., Radavich, K.A., Love, N.G., Ellis, M.W., Puri, I.K., 2011. Flame synthesis of carbon nanostructures on stainless steel anodes for use in microbial fuel cells. J. Power Sources 196, 5829–5834. doi:10.1016/j.jpowsour.2011.02.077

Luo, L., Li, D., Zang, J., Chen, C., Zhu, J., Qiao, H., Cai, Y., Lu, K., Zhang, X., Wei, Q., 2017. Polydopamine derived nitrogen-doped carbon coated magnesium ferrite nanofibers as anode material for lithium-ion batteries with enhanced cycling performance. Energy Technol. 5, 1364–1372. doi:10.1002/ente.201600686

Malvankar, N.S., Lovley, D.R., 2014. Microbial nanowires for bioenergy applications. Curr. Opin. Biotechnol. 27, 88–95. doi:10.1016/j.copbio.2013.12.003.

Miranda, R. de C.M. d., Gomes, E. de B., Pereira, N., Marin-Morales, M.A., Machado, K.M.G., Gusmão, N.B. de, 2013. Biotreatment of textile effluent in static bioreactor by Curvularia lunata URM 6179 and Phanerochaete chrysosporium URM 6181. Bioresour. Technol. 142, 361–367. doi:10.1016/j.biortech.2013.05.066

Munjal, M., Tiwari, B., Lalwani, S., Sharma, M., Singh, G., Sharma, R.K., 2020. An insight of bioelectricity production in mediator less microbial fuel cell using mesoporous Cobalt Ferrite anode. Int. J. Hydrogen Energy 45, 12525–12534. doi:10.1016/j.ijhydene.2020.02.184

Muthukumar, H., Mohammed, S.N., Chandrasekaran, N., Sekar, A.D., Pugazhendhi, A., Matheswaran, M., 2018. Effect of iron doped Zinc oxide nanoparticles coating in the anode on current generation in microbial electrochemical cells. Int. J. Hydrogen Energy 1–10. doi:10.1016/j.ijhydene.2018.06.046

Myers, C. R.. Nealson, K. H., 1990.Respiration-Linked Proton Translocation Coupled to Anaerobic Reduction of Manganese (IV) and Iron (III) in Shewanella putrefaciensMR-1.J. Bacteriol. 172, 6232−6238.

Narsimulu, D., Rao, B.N., Venkateswarlu, M., Srinadhu, E.S., Satyanarayana, N., 2016. Electrical and electrochemical studies of nanocrystalline mesoporous $MgFe_2O_4$ as anode material for lithium battery applications. Ceram. Int. 42, 16789–16797. doi:10.1016/j.ceramint.2016.07.168

Paisio, C.E., Talano, M.A., González, P.S., Busto, V.D., Talou, J.R., Agostini, E., 2012. Isolation and characterization of a Rhodococcus strain with phenol-degrading ability and its potential use for tannery effluent biotreatment. Environ. Sci. Pollut. Res. 19, 3430–3439. doi:10.1007/s11356-012-0870-8

Peng, X., Chu, X., Wang, S., Shan, K., Song, D., Zhou, Y., 2017. Bio-power performance enhancement in microbial fuel cell using Ni-ferrite decorated anode. RSC Adv. 7, 16027–16032. doi:10.1039/C7RA01253E

Permien, S., Indris, S., Scheuermann, M., Schürmann, U., Mereacre, V., Powell, A.K., Kienle, L., Bensch, W., 2015. Is there a universal reaction mechanism of Li insertion into oxidic spinels: A case study using $MgFe_2O_4$. J. Mater. Chem. A 3, 1549–1561. doi:10.1039/c4ta05054a

Pu, K.-B., Ma, Q., Cai, W.F., Chen, Q.-Y., Wang, Y.H., Li, F.-J., 2018. Polypyrrole modified stainless steel as high performance anode of microbial fuel cell. Biochem. Eng. J. 132, 255–261. doi:10.1016/j.bej.2018.01.018

Roy, U., Das, P., Bhowal, A., 2019. Treatment of azo dye (congo red) solution in fluidized bed bioreactor with simultaneous approach of adsorption coupled with biodegradation: optimization by response surface methodology and toxicity assay. Clean Technol. Environ. Policy 21, 1675–1686. doi:10.1007/s10098-019-01736-7

Sathishkumar, K., AlSalhi, M.S., Sanganyado, E., Devanesan, S., Arulprakash, A., Rajasekar, A., 2019, Sequential electrochemical oxidation and bio-treatment of the azo dye

congo red and textile effluent. Journal of Photochemistry and Photobiology B: Biology 200, 111655. doi.org/10.1016/j.jphotobiol.2019.111655

Sharari, M., Latibari, J., Guillet, A., Aurousseau, M., Mouhamadou, B., Rafeiee, G., Mirshokraei, A., Parsapaghouh, D., 2011. Application of the white rot fungus Phanerochaete chrysosporium in biotreatment of bagasse effluent. Biodegradation 22, 421–430. doi:10.1007/s10532-010-9415-3

Sultana, S., Khan, M. D., Sabir, S., Gani, K. M., Oves, M., and Khan, M. Z., 2015. Bio-electro degradation of azo-dye in a combined anaerobic–aerobic process along with energy recovery. New J. Chem. 39, 9461-9470

Sydow, A., Krieg, T., Mayer, F., Schrader, J., Holtmann, D., 2014. Electroactive bacteria—molecular mechanisms and genetic tools. Appl. Microbiol. Biotechnol. 98, 8481–8495. doi:10.1007/s00253-014-6005-z

Telke, A. A., Joshi, S. M., Jadhav, S. U., Tamboli, D. P., Govindwar, S. P., 2010. Decolorization and detoxification of Congo red and textile industry effluent by an isolated bacterium Pseudomonas sp. SU-EBT. Biodegradation 21, 283–296. DOI 10.1007/s10532-009-9300-0

Tholkappiyan, R., Vishista, K., 2015. Combustion synthesis of Mg–Er ferrite nanoparticles: Cation distribution and structural, optical, and magnetic properties. Mater. Sci. Semicond. Process. 40, 631–642.

Wang, R., Yan, M., Li, H., Zhang, L., Peng, B., Sun, J., Liu, D., Liu, S., 2018. FeS_2 Nanoparticles Decorated Graphene as Microbial-Fuel-Cell Anode Achieving High Power Density. Adv. Mater. 30, 1–7. doi:10.1002/adma.201800618

Ye, S., Zeng, G,. Wu, H., Liang, J., Zhang, C., Dai, J., Xiong, W., Song, B., Wu, S., Yu, J., 2019. The effects of activated biochar addition on remediation efficiency of co-composting with contaminated wetland soil. Resour Conserv Recy 140, 278-285. doi.org/10.1016/j.resconrec.2018.10.004

Ye, S., Zeng, G., Tan, X., Liang, J., Song, B., Tang, N., Zhang, P., Yang, Y., Chen, Q., Li, X., 2020. Nitrogen-doped biochar fiber with graphitization from Boehmeria nivea for promoted peroxymonosulfate activation and non-radical degradation pathways with enhancing electron transfer. Applied Catalysis B: Environmental 269, 118850, 1-11. doi.org/10.1016/j.apcatb.2020.118850

Yellappa, M., Sravan, J.S., Sarkar, O., Reddy, Y.V.R., Mohan, S.V., 2019. Modified conductive polyaniline-carbon nanotube composite electrodes for bioelectricity generation and waste remediation. Bioresour. Technol. 284, 148–154. doi:10.1016/j.biortech.2019.03.085

Yin, T., Zhang, H., Yang, G., Wang, L., 2019. Polyaniline composite TiO_2 nanosheets modified carbon paper electrode as a high performance bioanode for microbial fuel cells. Synth. Met. 252, 8–14. doi:10.1016/j.synthmet.2019.03.027

Yong, X.Y., Yan, Z.Y., Shen, H.B., Zhou, J., Wu, X.Y., Zhang, L.J., Zheng, T., Jiang, M., Wei, P., Jia, H.H., Yong, Y.C., 2017. An integrated aerobic-anaerobic strategy for performance enhancement of Pseudomonas aeruginosa-inoculated microbial fuel cell. Bioresour. Technol. 241, 1191–1196. doi:10.1016/j.biortech.2017.06.050.

Yuan, H., Deng, L., Chen, Y., Yuan, Y., 2016. MnO_2/Polypyrrole/MnO_2 multi-walled-nanotube-modified anode for high-performance microbial fuel cells. Electrochim. Acta 196, 280–285. doi:10.1016/j.electacta.2016.02.183

Zhang, Y., Sun, J., Hou, B., Hu, Y., 2011. Performance improvement of air-cathode

single-chamber microbial fuel cell using a mesoporous carbon modified anode. J. Power Sources. 196, 7458–7464. doi:10.1016/j.jpowsour.2011.05.004.

Zheng, S., Yang, F., Chen, S., Liu, L., Xiong, Q., Yu, T., Zhao, F., Schröder, U., Hou, H., 2015. Binder-free carbon black/stainless steel mesh composite electrode for high-performance anode in microbial fuel cells. J. Power Sources 284, 252–257. doi:10.1016/j.jpowsour.2015.03.014

Zhong, D., Liao, X., Liu, Y., Zhong, N., Xu, Y., 2018. Enhanced electricity generation performance and dye wastewater degradation of microbial fuel cell by using a petaline NiO@ polyaniline-carbon felt anode. Bioresour. Technol. 258, 125–134. doi:10.1016/j.biortech.2018.01.117